Simulation of the development of karst aquifers using a coupled continuum pipe flow model

Rudolf Liedl, Martin Sauter,[1] Dirk Hückinghaus, Torsten Clemens, and Georg Teutsch
Applied Geology, University of Tübingen, Tübingen, Germany

Received 24 January 2002; revised 6 November 2002; accepted 6 November 2002; published 14 March 2003.

[1] This paper is intended to provide insight into the controlling mechanisms of karst genesis based on an advanced modeling approach covering the characteristic hydraulics in karst systems, the dissolution kinetics, and the associated temporal decrease in flow resistance. Karst water hydraulics is strongly governed by the interaction between a highly conductive low storage conduit network and a low-conductive high-storage rock matrix under variable boundary conditions. Only if this coupling of flow mechanisms is considered can an appropriate representation of other relevant processes be achieved, e.g., carbonate dissolution, transport of dissolved solids, and limited groundwater recharge. Here a parameter study performed with the numerical model Carbonate Aquifer Void Evolution (CAVE) is presented, which allows the simulation of the genesis of karst aquifers during geologic time periods. CAVE integrates several important features relevant for different scenarios of karst evolution: (1) the complex hydraulic interplay between flow in the karst conduits and in the small fissures of the rock matrix, (2) laminar as well as turbulent flow conditions, (3) time-dependent and nonuniform recharge to both flow systems, (4) the widening of the conduits accounting for appropriate physicochemical relationships governing calcite dissolution kinetics. This is achieved by predefining an initial network of karst conduits (''protoconduits'') which are allowed to grow according to the amount of aggressive water available due to hydraulic boundary conditions. The increase in conduit transmissivity is associated with an increase in conduit diameters while the conductivity of the fissured system is assumed to be constant in time. The importance of various parameters controlling karst genesis is demonstrated in a parameter study covering the recharge distribution, the upgradient boundary conditions for the conduit system, and the hydraulic coupling between the conduit network and the rock matrix. In particular, it is shown that conduit diameters increase in downgradient or upgradient direction depending on the spatial distribution (local versus uniform) of the recharge component which directly enters the conduit system. *INDEX TERMS:* 1829 Hydrology: Groundwater hydrology; 1894 Hydrology: Instruments and techniques; *KEYWORDS:* karst hydrology, aquifer evolution, groundwater flow, pipe flow, calcite dissolution kinetics, numerical modeling

Citation: Liedl, R., M. Sauter, D. Hückinghaus, T. Clemens, and G. Teutsch, Simulation of the development of karst aquifers using a coupled continuum pipe flow model, *Water Resour. Res.*, *39*(3), 1057, doi:10.1029/2001WR001206, 2003.

1. Introduction

[2] Karstified limestone aquifers are characterized by highly varied hydraulic properties which are a result of the complex interactions between karst conduits, discrete fractures and the rock matrix [*Ford and Williams*, 1989]. Conduits are characterized by low storage and high flow velocities, while the discrete fissured system and the rock matrix display much higher storage and low flow velocities [*Atkinson*, 1977; *Teutsch*, 1988, 1989]. Due to this dual-porosity, dual-permeability structure of the carbonate medium the resulting parameters are difficult to interpret from standard investigation techniques such as hydraulic tests, and cannot be easily regionalized at the catchment scale [*Sauter*, 1991]. In order to provide additional spatial information on hydraulic parameters and their response at the catchment and sub-catchment scale, a new approach is presented. This approach requires the quantitative simulation of the calcite dissolution during geologic time periods including the recharge distribution as well as the definition of hydraulic and hydrochemical boundary conditions. The resulting parameter distribution can then be compared to field observations.

[3] A major process governing the genesis of karst aquifers is carbonate dissolution, whereby the fractures or conduits in the phreatic zone are enlarged with time due to the undersaturation of carbonate species [*Kaye*, 1957; *Weyl*, 1958]. Kinetics of calcite dissolution was studied by *Berner and Morse* [1974], *Plummer and Wigley* [1976], *Plummer et al.* [1978], and *Buhmann and Dreybrodt*

[1] Now at Geoscience Centre, University of Göttingen, Göttingen, Germany.

0043-1397/03/2001WR001206

[1985a, 1985b] who showed that, apart from film diffusion, other processes such as the dissolution rate at the reactive surface or the type of flow (turbulent or laminar) determine the dissolution of carbonate rocks. Based on data by *Plummer and Wigley* [1976], *White* [1977] introduced the kinetic trigger concept stating that the order of the dissolution rate increases for concentrations close to equilibrium so that Ca^{2+} saturation is approached more slowly. This explains why even fractures far from the recharge location can be enlarged. Overviews of limestone dissolution processes and their quantification including data from laboratory experiments and field observations are given by *Dreybrodt* [1998, 2000], *Dreybrodt and Eisenlohr* [2000], and *White* [2000].

[4] Based on the theoretical and laboratory work described above, early numerical models were developed to simulate the evolution of karst aquifers. Flow and carbonate dissolution in single conduits were described by *Dreybrodt* [1990, 1996], *Palmer* [1991, 2000], *Groves and Howard* [1994a], and *Dreybrodt and Gabrovšek* [2000]. *Groves and Howard* [1994b] and *Howard and Groves* [1995] also included the effect of laminar and turbulent flow conditions on the evolution of preferential flow paths in conduit networks exhibiting regular patterns, thus extending the investigations of *Lauritzen et al.* [1992]. Somewhat more irregular network structures generated by percolation algorithms were studied by *Siemers and Dreybrodt* [1998], *Kaufmann and Braun* [1999], *Dreybrodt and Siemers* [2000], and *Gabrovšek and Dreybrodt* [2000] who investigated the impact of several geometric and chemical parameters on the development of preferential flow paths during the early stage of karstification.

[5] All these studies only analyzed karst systems with flow in the conduit network and not in the adjacent fissured blocks, which at catchment scale represent most of the water storage, even in well karstified systems. To date, the purely hydraulic interaction between the fissured system and the conduit network has been simulated by employing three types of modeling approaches [*Teutsch and Sauter*, 1998]. Firstly, multiple sets of fractures may be coupled to each other in order to represent the different hydraulic properties of the fissured and the conduit system [e.g., *Dershovitz et al.*, 1991]. Alternatively, double-continuum or multicontinuum models have been applied where the cross-flow between the flow systems depends on the corresponding pressure differences via linear exchange terms [*Barenblatt et al.*, 1960; *Teutsch*, 1988, 1989; *Yilin et al.*, 1988; *Sauter*, 1992]. As a third approach, discrete networks of flow paths can be coupled to a continuum in order to model the dualistic flow patterns in karst systems (''hybrid models''). For steady state conductivities this technique has been introduced by *Kiraly* [1984] and *Yusun and Ji* [1988]. A qualitatively similar approach is presented by *MacQuarrie and Sudicky* [1996] who simulate pipe as well as open-channel flow in a drainage system which is connected to a continuum model of saturated/unsaturated flow.

[6] Apart from the double-continuum or multicontinuum approaches, several attempts have been undertaken during the past five years or so to combine karst flow models with a limestone dissolution model. The multiple fracture approach has been utilized by *Gabrovšek and Dreybrodt* [2001] who investigated a 2-D vertical scenario to predict the temporal variation of a karst water table under the influence of varied initial fracture system and different hydraulic boundary conditions. *Annable and Sudicky* [1998] investigate conduit growth for a vertical aquifer cross section under varied recharge conditions as a function of vertical fracture distribution. Saturated and variably saturated flow conditions were implemented in their approach to investigate open and closed P_{CO2} dissolution. The effects of initial conduit diameters, recharge and matrix heterogeneity on the development of 2-D horizontal conduit networks were studied by *Kaufmann and Braun* [2000]. In both of the above models, flow in the conduits is assumed to be laminar.

[7] The objective of this paper is to provide an extended analysis of controlling mechanisms of karst development. To this end, the modeling approach, which has been presented in a rather qualitative manner by *Liedl and Sauter* [1998] and *Sauter and Liedl* [2000], is augmented. In particular, a comprehensive compilation of quantitative relationships is given here, thus providing a theoretical basis for integrating the simulation of (1) groundwater flow in the fissured system and the conduit network based on the hybrid modeling approach which accounts for laminar and turbulent flow conditions in 1-D tubes in a 3-D network, (2) calcite dissolution kinetics and (3) the increase of hydraulic conductivity with time due to the dissolutional enlargement of the karst conduits.

[8] The paper is organized as follows: Section 2 is devoted to a qualitative description of flow, transport and dissolution processes in carbonate aquifers. In section 3 a comprehensive mathematical formulation of these processes and their interactions is provided. Finally, section 4 presents four examples demonstrating how the evolution of a dendritic conduit pattern is affected by varying the controlling hydraulic parameters. Here a dendritic network is studied in contrast to the genesis of a maze system discussed by *Clemens et al.* [1998].

2. Processes

[9] Figure 1 presents a conceptual diagram of a karstic landscape and aquifer system. As illustrated in Figure 1 the governing processes which are believed to control flow, transport and dissolution in a karst aquifer are also outlined. Regarding flow in the phreatic zone, two hydraulic systems can be distinguished: On the one hand, there is flow in the discrete system of larger fractures or conduits and, on the other hand, a Darcian flow system is provided by the rock matrix and smaller fissures.

[10] The conduit system is characterized by relatively high flow velocities but low storage capacity. Depending on the magnitude of the flow velocity, either laminar or turbulent flow may occur in individual tubes. Observations in natural karst systems show that turbulent flow is preferentially established in larger conduits [*Jeannin and Maréchal*, 1995]. For instance, if flow velocity in a circular conduit is assumed to be 50 m/h, turbulent flow sets in for a conduit diameter above 50 cm.

[11] The second hydraulic system can be visualized as a network of small fissures, which display a high degree of connectivity [*Sauter*, 1992]. This fissured system is charac-

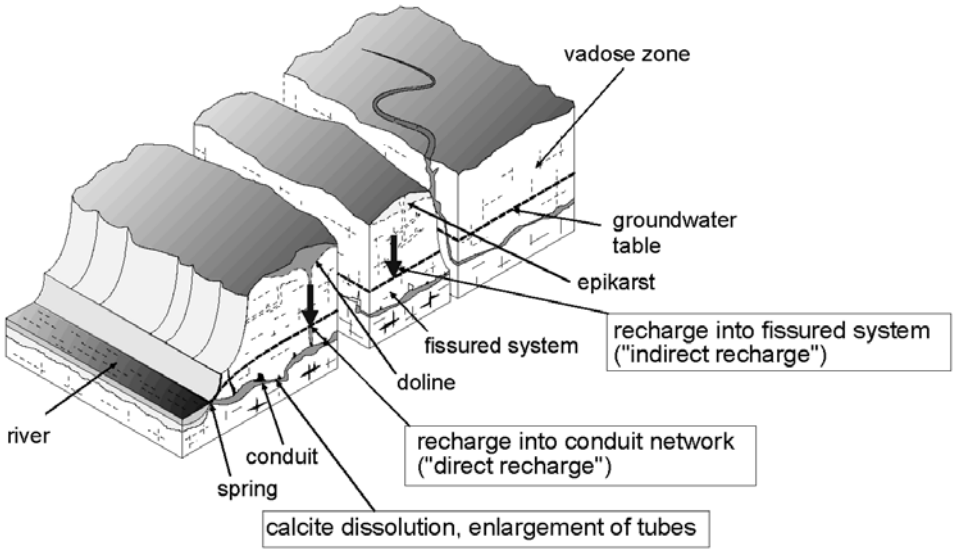

Figure 1. Conceptual model of a karst aquifer.

terized by a high storage but low flow velocities. Depending on the piezometric head difference between the fissured and the conduit system water is exchanged between these two systems.

[12] Focusing on the $CaCO_3$ system, calcite dissolution is found to occur at the conduit surfaces leading to the enlargement of conduit diameters. Dissolution rates depend on the flow regime and equilibrium concentration of dissolved Ca^{2+}. The growth of conduit diameters leads to an increase in hydraulic conductivity of the conduit system and thus higher flow rates. The degree of Ca^{2+} undersaturation is larger at higher flow rates (shorter residence times) and therefore dissolution rates are increased as well. Higher dissolution rates in turn lead to a further increase in conduit diameters and therefore to higher flow rates; thus a positive feedback mechanism is established between dissolution rates and flow rate enhancement.

[13] Groundwater recharge is characterized by two different mechanisms: (1) indirect or diffuse recharge infiltrating through the vadose zone relatively slowly along narrow pathways which finally enter the fissured system at the groundwater table and (2) direct recharge, whereby water collects in surface depressions or just below the surface and rapidly enters the phreatic conduit system via vertical shafts.

[14] Juxtaposed with the different types of recharge are disparate Ca^{2+} concentrations which are a result of residence time in the vadose zone, whereby recharge entering the fissured system displays high calcite concentrations ranging close to equilibrium. Water moving through vertical shafts is typified by considerable undersaturation with respect to Ca^{2+} when it reaches the conduits.

3. Mathematical Development

3.1. Groundwater Flow

[15] The underlying conceptual development for the mathematical model to simulate karst aquifer genesis is illustrated in Figure 2. A continuum and a pipe network are coupled in order to represent the dualistic hydraulic system described above.

[16] Flow in the fissured system is modeled by a continuum approach using the Boussinesq equation [*Bear and Verruijt*, 1987]:

$$\frac{\partial}{\partial x}\left(T_x \frac{\partial h_c}{\partial x}\right) + \frac{\partial}{\partial y}\left(T_y \frac{\partial h_c}{\partial y}\right) = S\frac{\partial h_c}{\partial t} - r_c - \gamma \qquad (1)$$

where x, y are the space coordinates [L], t is time [T], h_c is the hydraulic head in the fissured system [L], T_x, T_y are the

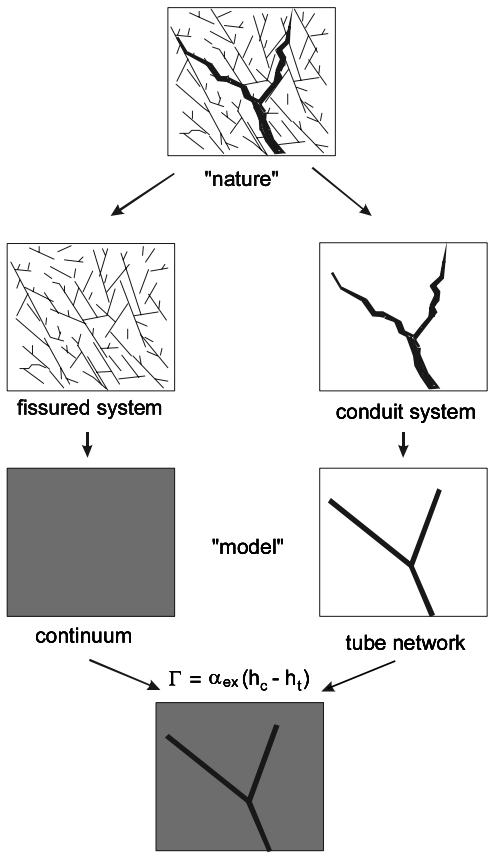

Figure 2. General model approach illustrating the fissured system simulated as a continuum and the karst conduits simulated as a tube network.

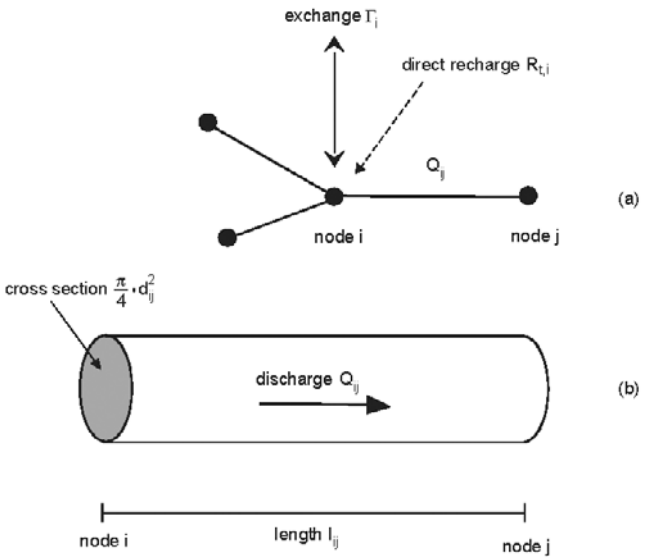

Figure 3. Flow in the conduit system: (a) pipe network and (b) single tube.

transmissivities along coordinate axes [L^2/T], S is the storage coefficient [-], r_c is the recharge into the fissured system per unit area [L/T] and γ represents the volumetric rate of fluid transfer between the fissured and the conduit system per unit area [L/T]. It may be noted that equation (1) can be adapted to confined and unconfined flow by appropriately defining aquifer transmissivities.

[17] The conduit system is modeled as a pipe network consisting of cylindrical tubes. It is assumed that the fluid within the network is incompressible. Head losses by expansion, constrictions and bending in the conduit system are assumed to be negligible. For the purpose of the simulations presented below, fully saturated flow conditions are assumed explicitly.

[18] At any node (point of intersection of tubes) i of the conduit network (Figure 3a) the conservation of volume is expressed by Kirchhoff's law [*Horlacher and Lüdecke*, 1992]

$$0 = \sum_j Q_{ij} + R_{t,i} + \Gamma_i \tag{2}$$

where Q_{ij} is the discharge of the tube connecting nodes i and j [L^3/T], $R_{t,i}$ is the direct recharge into node i [L^3/T], and Γ_i is the exchange flow rate between node i and the fissured system [L^3/T].

[19] For each tube, the discharge can be related to the head difference in the tube Δh_t [L], by applying the Darcy-Weisbach equation [*Bobok*, 1993]:

$$\Delta h_t = -\lambda \frac{l}{d} \frac{u|u|}{2g} \tag{3}$$

where λ is the friction factor [-], d is the pipe diameter [L], l is the length of the tube [L], $u = 4Q/(\pi\, d^2)$ is the average velocity [L/T] and g is the earth's gravitational acceleration [L/T^2], where the indices of the nodes have been omitted for simplicity. The friction factor λ depends on the velocity in the pipe via the Reynolds number $Re = ud/\nu$; with ν the kinematic viscosity [L^2/T] of water. For low flow velocities, i.e., $Re < 2300$, laminar flow is assumed and the Hagen-Poiseuille equation can be applied. The friction factor for laminar flow is calculated as

$$\lambda = \frac{64\ \nu}{d\ u} \tag{4}$$

This expression can be substituted in equation (3) and the discharge Q passing through a cross section of the pipe (Figure 3b) can be calculated as

$$Q = -\frac{\pi d^4 \Delta h_t g}{128 l \nu} \tag{5}$$

Experimental observations show that for turbulent flow ($Re \geq 2300$) the implicit Colebrook-White law is applicable [*Streeter and Wylie*, 1983; *Bobok*, 1993]

$$\frac{1}{\sqrt{\lambda}} = -2\log\left(\frac{2.51}{\mathrm{Re}\sqrt{\lambda}} + \frac{k}{3.71d}\right) \tag{6}$$

with pipe roughness k [L]. According to *Horlacher and Lüdecke* [1992] the discharge Q for turbulent flow is then given by

$$Q = -\sqrt{\frac{|\Delta h_t| g d^5 \pi^2}{2l}} \log\left(\frac{2.51\nu}{\sqrt{\frac{2|\Delta h_t| g d^3}{l}}} + \frac{k}{3.71d}\right) \cdot \frac{\Delta h_t}{|\Delta h_t|} \tag{7}$$

[20] The fissured and the conduit system are coupled at common nodes by a quasi-steady-state exchange term [*Barenblatt et al.*, 1960]. For each node of the network we can write, again omitting the index i,

$$\Gamma = \alpha_{ex}(h_c - h_t) \tag{8}$$

where α_{ex} is the exchange coefficient [L^2/T]. Thus the exchange coefficient is equivalent to the volumetric rate of fluid transferred between the two hydraulic systems for a unit head difference.

[21] The distribution of total recharge into the fissured and the conduit system may vary in space. Considering numerical solution approaches, which are based on the discretization of the model domain, weighting factors ω ($0 \leq \omega \leq 1$) accounting for the fraction of direct recharge are attributed to each model cell. Therefore, if R [L^3/T] denotes the total recharge into a model cell, the recharge into the corresponding tube is $R_t = \omega\, R$, while $R_c = (1 - \omega)\, R$ is the recharge allocated to the continuum. It should be noted that the weighting factor ω depends inversely proportional on cell size if the amount of direct recharge R_t is assumed to be fixed.

3.2. Ca^{2+} Transport and Calcite Dissolution

[22] In the modeling approach only transport of Ca^{2+} within the conduit network is considered. For each tube, transport of Ca^{2+} ions is modeled by the one-dimensional advection equation

$$\frac{\partial c}{\partial t} = \frac{A}{V} F - u \frac{\partial c}{\partial x} \tag{9}$$

where c is the Ca^{2+} concentration [M/L^3] in the tube, A is the surface of the tube [L^2], V is the bulk volume [L^3] and F =

$F(c)$ is the dissolution rate of calcite [M/(L^{2}T)]. In the literature a number of relationships have been published [e.g., *Plummer and Wigley*, 1976; *Plummer et al.*, 1978; *Palmer*, 1984, 1988; *Dreybrodt*, 1988, 1985b] which allow the quantification of carbonate dissolution rates $F(c)$.

[23] For the examples presented in section 4, the dissolution rate $F = F(c)$ is quantified according to *Buhmann and Dreybrodt* [1985a]. For Ca^{2+} concentrations far from equilibrium a linear rate law applies, i.e.

$$F(c) = \alpha(x)\left(c_{eq} - c\right) \tag{10}$$

for $c < k_{sw} c_{eq}$ where k_{sw} denotes the relative concentration of which dissolution rates change from low to high order. The rate constant $\alpha(x)$ [L/T] in equation (10) is given by

$$\alpha(x) = \begin{cases} \alpha_{lam}\left(1 + \dfrac{\alpha_{lam} d(x)}{D}\right)^{-1} & \text{for } Re \le 2300 \\ \alpha_{tur} & \text{for } Re > 2300 \end{cases} \tag{11}$$

where α_{lam} and α_{tur} stand for the kinetic rate constants [L/T] for laminar and turbulent flow conditions, respectively. For laminar flow ($Re = 2300$) the term in parentheses considers mass transport by diffusion for large tube diameters d depending on the positions x along the conduit. D represents the coefficient of diffusion [L^2/T] of Ca^{2+} in water. For Ca^{2+} concentrations close to equilibrium ($c > k_{sw} c_{eq}$) a fourth-order rate law is utilized, i.e.

$$F(c) = \beta\left(c_{eq} - c\right)^4 \tag{12}$$

with β = kinetic rate constant for the fourth-order reaction [L^{10}/(M^{3}T)].

[24] The increase of the tube diameter due to calcite dissolution can be calculated by considering the conservation of mass. For a time interval Δt the increase Δd of the tube diameter is derived from mass balance considerations and is expressed as

$$\Delta d = \frac{2|Q|}{d\pi l} \frac{\Delta c \Delta t}{\rho_{Ca}} \tag{13}$$

with Δc concentration difference between outlet and inlet of the tube [M/L^3] and ρ_{Ca} the density of the carbonate rock [M/L^3].

[25] As a first approximation, total mixing of waters is assumed at tube intersections. With recharge into the conduit system via vertical shafts and exchange water derived from the fissured system as source terms, the Ca^{2+}concentration c_i at node i is obtained by the weighted arithmetic mean of the single flow components (Figure 3a)

$$c_i = \frac{\sum_j Q_{ij}^+ c_i + \Gamma_i^+ c_{ex,i} + R_i\ c_{re,i}}{\sum_j Q_{ij}^+ + \Gamma_i^+ + R_i} \tag{14}$$

where $Q_{ij}^+ = \max\{Q_{ij}, 0\}$, $\Gamma_i^+ = \max\{\Gamma_i, 0\}$, $c_{ex,i}$ is the Ca^{2+} concentration of exchange water [M/L^3] and $c_{re,i}$ is the Ca^{2+} concentration of direct recharge [M/L^3] at node i. In equation (14) the quantities Q_{ij}^+ and Γ_i^+ have to be used instead of Q_{ij} and Γ_i because only waters flowing towards the node i contribute to the mixing. The resulting concentration c_i serves as a boundary value for the tubes which are located downgradient from node i. The Ca^{2+} concentration of the fissured system is assumed to be a fixed value (e.g., $c_{ex} = 0.9\ c_{eq}$). This implies that geochemical reactions in the fissured system (matrix blocks) are not explicitly modeled although the blocks may have received waters of different origin. A constant value of c_{ex} is a state-of-the-art assumption also used by other authors [*Kaufmann and Braun*, 2000].

3.3. Model Implementation

[26] Based on the theory outlined above the numerical model Carbonate Aquifer Void Evolution (CAVE) has been programmed to simulate the evolution of karst aquifers for different boundary conditions [*Hückinghaus*, 1998; *Clemens*, 1997]. The main numerical solution approach implemented in CAVE is briefly summarized in this subsection.

[27] Flow in the fissured system is calculated by a finite difference scheme using MODFLOW [*McDonald and Harbaugh*, 1988]. The equations for the conduit network generally constitute a nonlinear system which has to be solved iteratively, e.g., by the Newton-Raphson technique [*Press et al.*, 1992] which is implemented in CAVE. Flow conditions in each tube are allowed to change from turbulent to laminar or vice versa within each time step.

[28] Both hydraulic systems are coupled via equation (8). This coupling is implemented by alternately solving for the heads in the fissured system and the heads at the nodes of the conduit network. By updating head values after each step another iteration cycle is established.

[29] After convergence of this loop, which is tantamount to a "trade off" of flows in both hydraulic systems, the advective transport of Ca^{2+} in each tube is computed by solving equation (9) with a semi-analytical upwind finite-difference scheme. The tubes are divided into several segments of uniform length and for each segment the increase in concentration during the corresponding residence time interval is obtained by an exact integration of equation (9) for the dissolution rate $F(c)$ specified according to equations (10)–(12). The analytical integration ensures this approach to be mass conservative and unaffected by the Courant criterion. Next, the increase in segment diameter is calculated using equation (13). These diameters are then used to obtain an equivalent tube diameter for pipe flow modeling along the entire length of each tube in the next time step. This equivalent diameter $\bar{d}$ is chosen such that the discharge is the same as in the nonuniform tube for the given head gradient. For laminar flow we obtain

$$\bar{d} = \left. l \middle/ \sum_j \frac{l_j}{d_j^4} \right)^{\frac{1}{4}} \tag{15}$$

where l_j is the length and d_j is the diameter of the tube segment j. For turbulent flow conditions the equivalent tube diameter is obtained by iteratively solving equation (7) according to the Newton-Raphson method mentioned above.

4. Model Results and Discussion

[30] Below, four examples are presented in order to demonstrate some of the salient karst development processes covered by the numerical model presented above. In particular, fixed-head boundary conditions at upstream ends

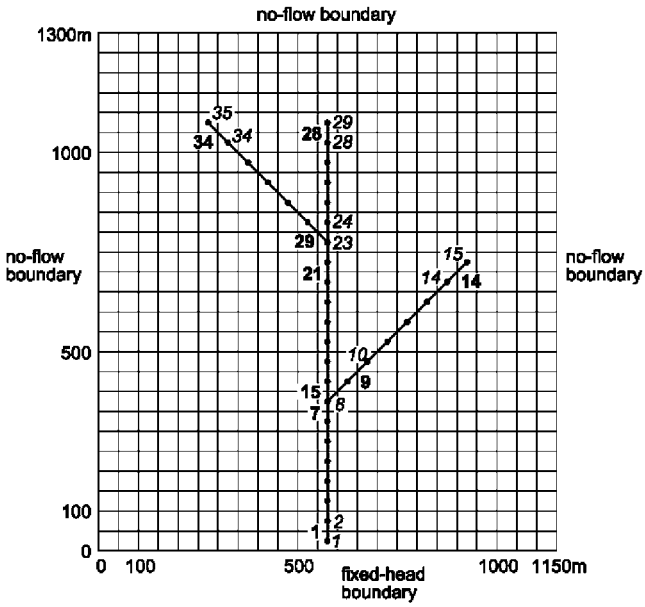

Figure 4. Configuration of the network used for model simulations. Numbers indicate nodes (italic) and tubes (bold face).

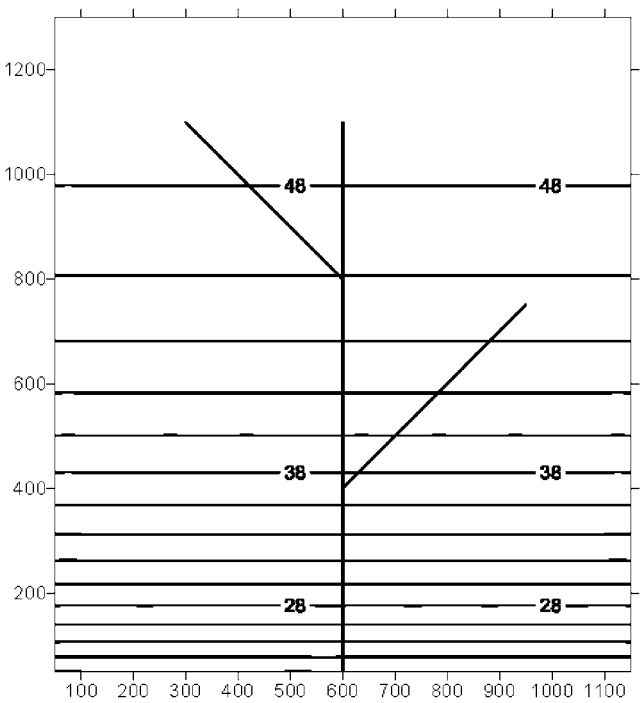

Figure 5. Potentials at the beginning of the simulations.

of the conduit network, varying exchange rates of water between the fissured and the conduit system and varied recharge conditions which affect conduit development patterns are evaluated.

[31] The modeled domain employed for these simulations measures 1250 m by 1150 m in 2-D plan section and is shown in Figure 4. Three sides of the modeling domain are no-flow boundaries and the fourth is a constant head boundary with hydraulic heads of 20 m, representing a river. The initial conduit system (''protoconduits'') consists of 34 tubes with 1 mm in diameter which is in the range of frequently measured fracture apertures in limestones not affected by karstification [*Motyka and Wilk*, 1984; *Böcker*, 1969]. The recharge data and the hydraulic parameters used in the example are typical values derived from a karst aquifer system in SW Germany [*Sauter*, 1992]. The hydraulic conductivity of the fissured system used throughout the simulations is fixed at 1.0×10^{-5} m/s. A constant recharge rate of 400 mm/yr is applied evenly throughout the top surface of the modeling domain. It is assumed that the aquifer is unconfined and the water within the fissured system shows a certain degree of undersaturation ($c = 0.9\ c_{eq}$). The hydraulic potentials in the fissured system at the beginning of the simulations are shown in Figure 5.

[32] For quantifying limestone dissolution according to equations (10)–(12) the following data are used in the model runs discussed below: $c_{eq} = 2 \times 10^{-3}$ mol/L, $\alpha_{lam} = 2.5 \times 10^{-5}$ cm/s, $\alpha_{tur} = 5 \times 10^{-5}$ cm/s, $\beta = 1.2 \times 10^{13}$ cm^{10}/(mol^3 s), $D = 10^{-5}$ cm^2/s and $k_{sw} = 0.9$ [*Dreybrodt*, 1988]. The value of c_{eq} does not change with time, i.e., the system (unconfined aquifer) is assumed to be open with respect to CO_2.

4.1. Simulation of Decoupled Conduit and Fissured System

[33] In this simulation (scenario 1) the conduit system and the fissured system are assumed to be hydraulically independent from each other (i.e., $\alpha_{ex} = 0$ m^2/s). Constant head values are specified such that $h_t = 48.96$ m at nodes 15 and 29 and $h_t = 45.19$ m at node 35 (Figure 4). These constant head values correspond to the initial heads in the fissured system whose isolines are depicted in Figure 5. Since the two hydraulic systems are decoupled from each other, the potentials in the fissured system do not change during the simulation period. The enlargement of the conduit system propagates from the upstream constant head boundaries in direction of the spring which is shown in Figure 6 for the conduit segment between nodes 1 and 15 (Figure 4). The reason for this is the inflowing water which is highly undersaturated with respect to calcite at the nodes 15, 29, and 35 (direct recharge, e.g., from vertical shafts) leading to high dissolution rates at the water inlets. At the beginning of the simulation, the enlargement of the conduits occurs almost exclusively due to the slow fourth-order kinetics; and the penetration length of the water to reach

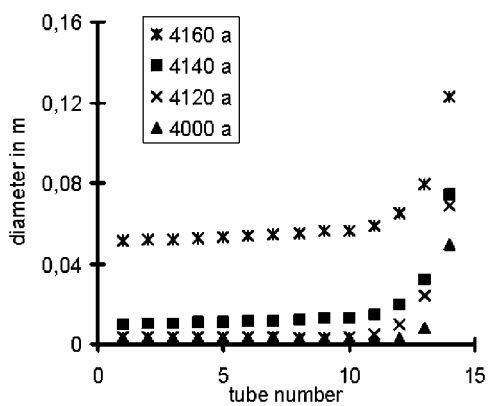

Figure 6. Diameters of tubes 1–14 for scenario 1 (legend denotes simulation times).

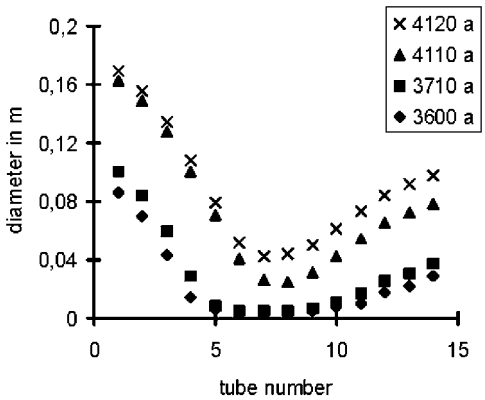

Figure 7. Diameters of tubes 1–14 for scenario 2 (legend denotes simulation times).

90% saturation is rather short. After 3900 years the penetration length for first-order kinetics increases noticeably and finally reaches the spring after 4130 years when the "breakthrough" [*Dreybrodt*, 1990] is achieved. The first branch of the conduit system to experience breakthrough is the shortest one (tubes 1–14). The discharge through these tubes increases and the flow conditions change from laminar to turbulent. The next branch of the conduit system that evolves is the center one (tubes 15–28).

[34] The simulation was terminated after 4830 years. At this time, the spring discharge reached 20 m^3/s which is approximately three orders of magnitude larger than at the beginning of the simulation. However, the observed increase in flow is not rationally based as this would imply an infinite reservoir providing water to the aquifer through nodes 15, 29 and 35. This emphasizes the inappropriateness of fixed head boundary conditions at the upgradient nodes of the conduit network except during initial stages of karst genesis. More realistic upgradient boundary conditions for the conduit network are examined in the following simulations.

4.2. Simulation of Fluid Exchange Between Conduit and Fissured Systems

[35] Building on the observations of the simulation results presented above, the influence of water exchange between the fissured system and the conduit system is studied by choosing an exchange coefficient of 10^{-4} m^2/s. In this simulation (scenario 2), the enlargement of the conduit system is simultaneously initiated at the spring and at the constant head boundaries at the upgradient ends of the conduit system (Figure 7).

[36] As in the first simulation, the enlargement of the conduits at the upgradient constant head boundaries are controlled by calcite dissolution due to highly undersaturated water entering the conduit system. The combination of the low hydraulic conductivity in the central part of the conduit system (tubes 15 to 22), the high hydraulic conductivity near the upstream end of the left branch and the fixed head condition at node 35 results in a head buildup in the left branch (Figures 8 and 9). A negative head difference $h_c - h_t$ develops and water flows from the tubes into the fissured system. This kind of flow configuration is only possible because water exchange between the two flow systems is allowed in this simulation.

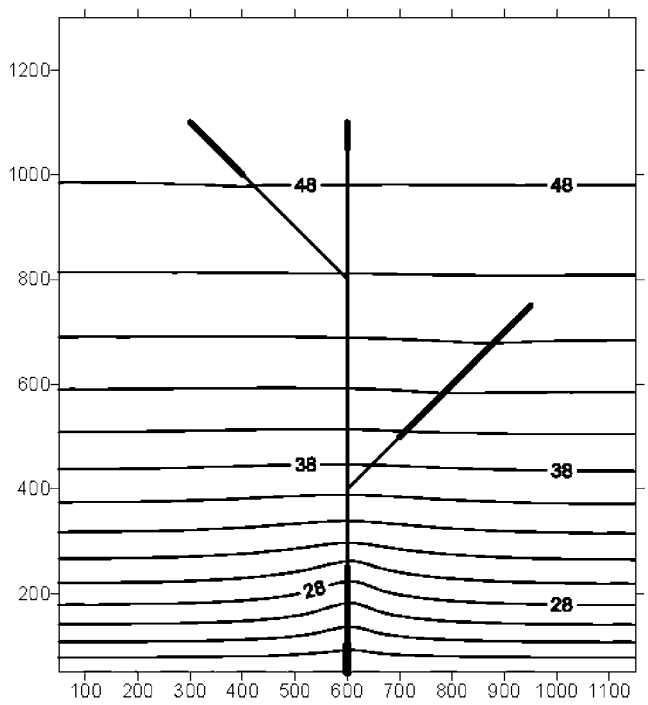

Figure 8. Potentials of the fissured system for scenario 2 after 3710 years. The thick lines show diameters larger than 0.01 m and 0.1 m (head values and coordinates in m).

[37] Close to the spring, i.e., near node 1 (Figures 8 and 9), the situation is somewhat different. In this region the flow rate in the conduit system increases in flow direction and the residence time of the water is reduced

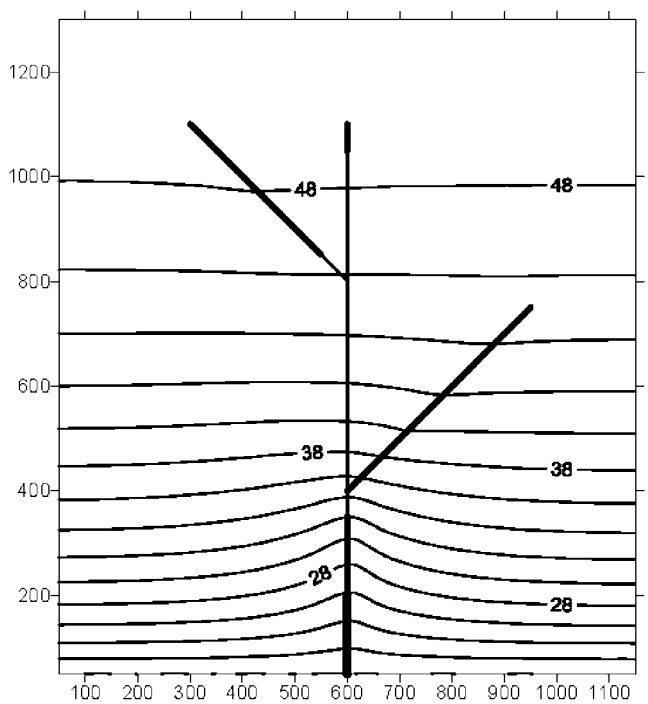

Figure 9. Potentials of the fissured system for scenario 2 after 4120 years. The thick lines show diameters larger than 0.01 m and 0.1 m (head values and coordinates in m).

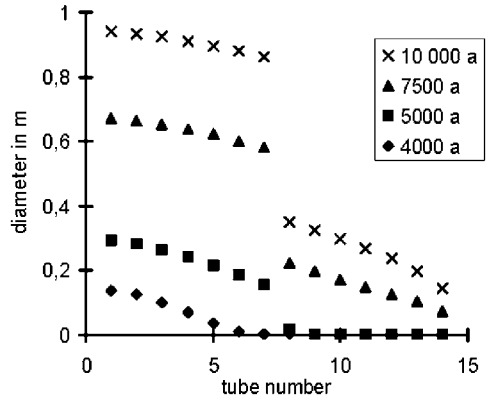

Figure 10. Diameters of tubes 1–14 for scenario 3 (legend denotes simulation times).

leading to an enhanced dissolution of calcite and faster growing conduits. Therefore the transmissivity of flow in the conduits close to the spring increases, the heads in the tubes decrease and a positive head difference $h_c - h_t$ occurs (Figures 8 and 9) so that water from the fissured system is re-entering the tubes. Breakthrough time for the tubes 1–14 (Figure 9) is achieved at 4110 years as compared to 4130 years from the first simulation, which is a result of the similarly slow enlargement of the conduits close to the bifurcation at node 8 controlling flow through the network. The simulation was stopped after 4660 years when the discharge at the spring exceeded 20 m^3/s.

4.3. Simulation of Conduit Evolution Without Fixed Recharge Heads

[38] In this example (scenario 3), fixed-head conditions are not specified at the nodes 15, 29 and 35 where artificially enhanced recharge was considered in previous simulations. Alternatively, nodes 15, 29 and 35 are dynamically connected to the fissured system by a linear exchange term according to equation (8) where $\alpha_{ex} = 10^{-4}$ m^2/s. In this simulation, carbonate dissolution is solely determined by the almost saturated water ($c = 0.9\ c_{eq}$) derived from the fissured system. Therefore only slow fourth-order kinetics was observed. The diameters of the right branch of the conduit system (tubes 1–14 in Figure 4) are depicted in Figure 10 illustrating a gradual increase in conduit diameters in the direction of the spring with time.

[39] The difference in diameters of tubes 7 and 8 for later times as illustrated in Figure 10 is a result of the difference in hydraulic gradients between the two branches. Whereas the tubes in the center branch (tubes 15–28) have a length of 50 m and are positioned in parallel to the mean groundwater flow direction, the tubes in the right branch (tubes 8–14) have a length of 70.71 m and are partly oriented oblique to the mean groundwater flow direction of the fissured system. Therefore the enlargement of the center branch proceeds more rapidly than that of the right branch as a function of the mean flow gradient (Figure 11).

[40] Due to the low flow resistance in the enlarged conduit system the heads in the fissured system decrease with time (Figures 11 and 12). The changes in the heads of the fissured system are much more pronounced than in the

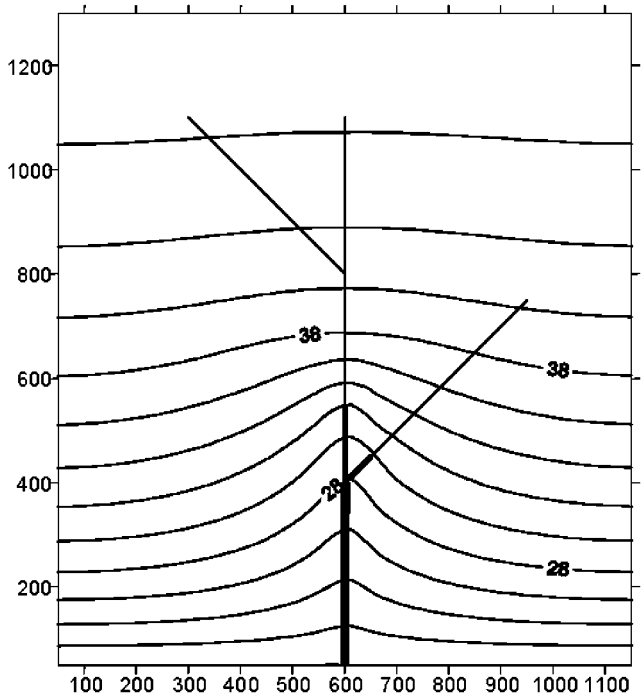

Figure 11. Potentials of the fissured system for scenario 3 after 5010 years. The thick lines show diameters larger than 0.01 m and larger than 0.1 m (head values and coordinates in m).

first and the second simulation since controlling head values for recharge were not specified a priori. Therefore no additional waters, apart from recharge, enters the model domain in the current simulation and the fissured system is

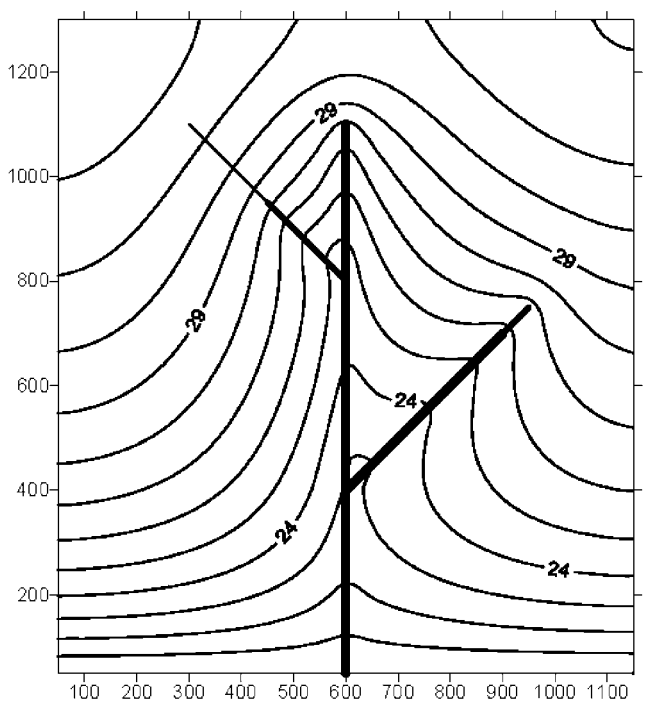

Figure 12. Potentials of the fissured system for scenario 3 after 7500 years. The thick lines show diameters larger than 0.01 m and larger than 0.1 m (head values and coordinates in m).

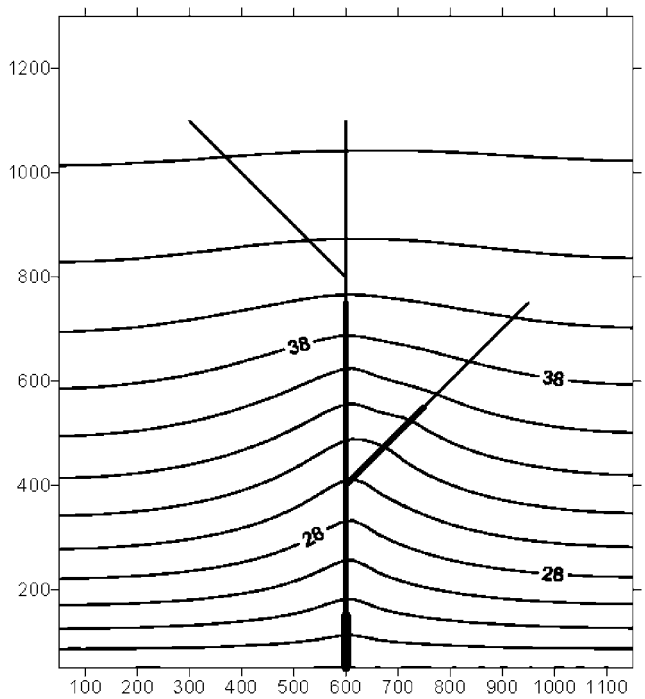

Figure 13. Potentials of the fissured system for scenario 4 after 1010 years. The thick lines show diameters larger than 0.01 m and larger than 0.1 m (head values and coordinates in m).

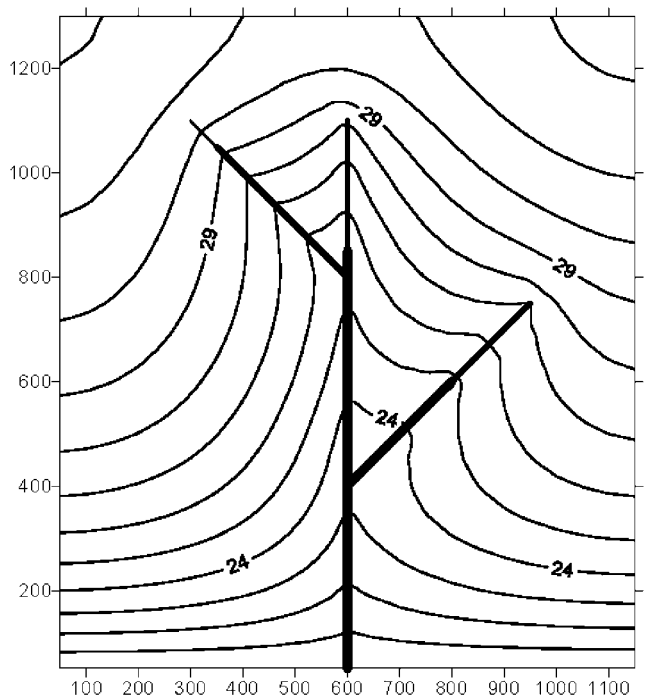

Figure 14. Potentials of the fissured system for scenario 4 after 1400 years. The thick lines show diameters larger than 0.01 m and larger than 0.1 m (head values and coordinates in m).

drained by the conduit network to a larger degree as is illustrated in Figures 11 and 12 for simulation times of 5000 years and 7500 years.

4.4. Simulation of Distributed Recharge

[41] The final simulation presented (scenario 4) considers the impact of direct recharge on karst development. The third simulation is slightly modified so that 1% of the total recharge is uniformly distributed to the nodes of the conduit system with a Ca^{2+} concentration of 1.2 mmol/L. The evolution of the conduit system and head distributions in the fissured system are shown in Figures 13 and 14 for 1010 years and 1400 years respectively.

[42] At the beginning of the simulation, the conduits are exclusively enlarged by fourth-order dissolution kinetics. Due to the specification of direct recharge, fast first-order dissolution starts to occur close to the water inlet locations of each tube. With the increase in spring discharge due to the growing diameter of conduits, the penetration length for the fast first-order dissolution propagates farther downgradient in each tube as is illustrated in Figure 15. At the beginning of the simulation, the largest hydraulic gradient is observed in tube number 1 next to the constant head boundary (i.e., at the spring). Therefore this tube is the first to experience breakthrough (after 640 years), i.e., first-order dissolution prevails throughout the tube. After breakthrough, the flow increases rapidly and changes from laminar to turbulent conditions. Consequently, dissolution rates are increased considerably leading to larger conduit diameters. Therefore the hydraulic gradient in tube number 1 decreases. The position of the largest gradient and therefore largest dissolution rate propagates from the spring in an upgradient fashion. These results extend the findings of *Clemens et al.* [1996] obtained for a simpler model geometry.

[43] After the enlargement reaches the bifurcation (node 8) both branches of the conduit system are enlarged simultaneously as in the previous simulation (Figure 15). However, due to the specification of direct recharge, highly undersaturated water reaches the conduit system diminishing the differences in tube diameters.

[44] The results of the current simulation illustrate that the enlargement of the conduit system propagates further upgradient step by step (Figure 15) whereas in the previous simulation the enlargement is more uniform in the whole conduit system because of slow fourth-order dissolution. The change of the kinetics in the current simulation from fourth to the fast first-order is responsible for the increased

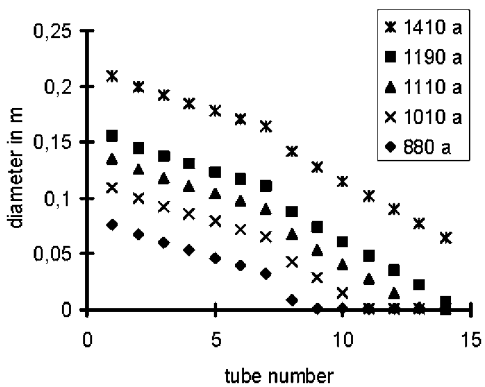

Figure 15. Diameters of tubes 1–14 for scenario 4 (legend denotes simulation times).

rapid evolution of the conduit system as compared to that of the previous simulation.

5. Conclusions

[45] In order to simulate the evolution of a karst aquifer a model has been developed which couples the flow in the fissured system with the flow in the conduit system. Furthermore the dissolution kinetics of calcite is taken into account. The model developed allows for the simulation of a variety of scenarios including different types of boundary conditions, direct recharge into the conduit system in addition to exchange of water between the fissured system and the conduit system.

[46] Several numerical experiments for a dendritic conduit network were presented to address issues related to boundary conditions and their effects on conduit evolution. Simulations with constant head boundaries at the upgradient ends of the conduit system show a faster enlargement of the tube diameters close to the spring and at the upstream constant head boundaries if the network is not hydraulically coupled to the high storage fissured system. In the cases where fluid exchange between the fissured and the conduit system was permitted, an enhanced widening of tubes was also observed close to the spring.

[47] In the cases where constant head boundaries were not specified at the upgradient ends of the conduit system, the enlargement of the conduit system has a dramatic effect on the hydraulic potentials of the systems simulated as artificially high heads were not considered for recharge and the fissured system was allowed to be drained by the conduit system. When recharge is completely routed to the fissured system, the diameters of the tubes gradually increase in a downgradient direction. In the simulations presented in sections 4.1–4.3, the water reaches the spring with Ca^{2+} concentrations near saturation.

[48] Direct recharge also plays an important role for the enlargement of karst conduits as presented in the last simulation. If a part of the undersaturated recharge is allocated directly to the conduit system, an accelerated enlargement of the conduit diameters is simulated. In contrast to the previous case the diameters of the tubes in the conduit system do not gradually increase. The conduit system evolves stepwise in an upgradient direction due to subsequent breakthroughs in adjacent tubes. The concentrations of Ca^{2+} at the spring are close to equilibrium at the beginning of the simulation and decrease after the breakthrough of the first tube is occurred.

[49] The results of the simulations presented illustrate that different boundary conditions may lead to different types of evolution of the conduit system. Furthermore, the time scales for the development of karst aquifers are highly dependent on these conditions. Due to the sensitivity of the evolution of the conduit system as related to boundary conditions, it is clear that boundary conditions and recharge distribution have to be selected carefully for model applications. In a further study the influence of parameters, which represent geological, hydraulic and climatic factors of karstification, on the duration of karst evolution for different modeling approaches will be examined.

[50] **Acknowledgments.** The studies were supported by the Deutsche Forschungsgemeinschaft (DFG) as a part of the Collaborative Research Center 275 (Sonderforschungsbereich 275) and by the European Union (contract CEC EV5V-CT94-0471).

References

Annable, W., and E. A. Sudicky, Simulation of karst genesis: Hydrodynamic and geochemical rock-water interactions in partially-filled conduits, *Bull. Hydrogéol.*, *16*, 211–221, 1998.

Atkinson, T. C., Diffuse flow and conduit flow in a limestone terrain in the Mendip Hills, Somerset, *J. Hydrol.*, *19*, 323–349, 1977.

Barenblatt, G. K., I. P. Zheltov, and N. Kochina, Basic concepts in the theory of seepage of homogeneous liquids in fissured rocks, *Prikl. Mat. Mekh.*, *24*(5), 852–864, 1960.

Bear, J., and A. Verruijt, *Modeling Groundwater Flow and Pollution*, 414 pp., D. Reidel, Norwell, Mass., 1987.

Berner, R. A., and J. W. Morse, Dissolution kinetics of calcium carbonate in sea water, IV, Theory of calcite dissolution, *Am. J. Sci.*, *274*, 108–134, 1974.

Bobok, E., *Fluid Mechanics for Petroleum Engineers*, 400 pp., Elsevier Sci., New York, 1993.

Böcker, T., Karstic water research in Hungary, *Bull. lnt. Assoc. Sci. Hydrol.*, *14*(4), 7–20, 1969.

Buhmann, D., and W. Dreybrodt, The kinetics of calcite dissolution and precipitation in geologically relevant situations of karst areas, 1, Open systems, *Chem. Geol.*, *48*, 189–211, 1985a.

Buhmann, D., and W. Dreybrodt, The kinetics of calcite dissolution and precipitation in geologically relevant situations of karst areas, 2, Closed systems, *Chem. Geol.*, *53*, 109–124, 1985b.

Clemens, T., Simulation der Entwicklung von Karstaquiferen, Ph.D. thesis, Fac. of Geosci., Univ. of Tübingen, Tübingen, Germany, 1997.

Clemens, T., D. Hückinghaus, M. Sauter, R. Liedl, and G. Teutsch, A combined continuum and discrete network reactive transport model for the simulation of karst development, *IAHS Publ.*, *237*, 309–318, 1996.

Clemens, T., D. Hückinghaus, M. Sauter, R. Liedl, and G. Teutsch, Simulation of the evolution of maze caves, *Bull. Hydrogéol.*, *16*, 201–209, 1998.

Dershovitz, W., P. Wallmann, and S. Kindred, Discrete fracture network modeling for the Stripa characterization and validation drift inflow predictions, *SKB Rep. 91-16*, Swed. Nucl. Power and Waste Manage. Co., Stockholm, 1991.

Dreybrodt, W., *Processes in Karst Systems*, 288 pp., Springer-Verlag, New York, 1988.

Dreybrodt, W., The role of dissolution kinetics in the development of karst aquifers in limestone: A model simulation of karst evolution, *J. Geol.*, *98*, 639–655, 1990.

Dreybrodt, W., Principles of early development of karst conduits under natural and man-made conditions revealed by mathematical analysis of numerical models, *Water Resour. Res.*, *32*(9), 2923–2935, 1996.

Dreybrodt, W., Limestone dissolution in karst environments, *Bull. Hydrogéol.*, *16*, 167–183, 1998.

Dreybrodt, W., Equilibrium chemistry of karst water in limestone terranes, in *Speleogenesis—Evolution of Karst Aquifers*, edited by A. B. Klimchouk et al., pp. 126–135, Natl. Speleol. Soc., Huntsville, Ala., 2000.

Dreybrodt, W., and L. Eisenlohr, Limestone dissolution rates in karst environments, in *Speleogenesis—Evolution of Karst Aquifers*, edited by A. B. Klimchouk et al., pp. 126–135, Natl. Speleol. Soc., Huntsville, Ala., 2000.

Dreybrodt, W., and F. Gabrovšek, Dynamics of the evolution of single karst conduits, in *Speleogenesis—Evolution of Karst Aquifers*, edited by A. B. Klimchouk et al., pp. 184–193, Natl. Speleol. Soc., Huntsville, Ala., 2000.

Dreybrodt, W., and J. Siemers, Cave evolution on two-dimensional networks of primary fractures in limestone, in *Speleogenesis—Evolution of Karst Aquifers*, edited by A. B. Klimchouk et al., pp. 201–211, Natl. Speleol. Soc., Huntsville, Ala., 2000.

Ford, D. C., and P. W. Williams, *Karst Geomorphology and Hydrology*, 601 pp., Chapman and Hall, New York, 1989.

Gabrovšek, F., and W. Dreybrodt, Role of mixing corrosion in calcite-aggressive H_2O-CO_2-$CaCO_3$ solutions in the early evolution of karst aquifers in limestone, *Water Resour. Res.*, *36*(5), 1179–1188, 2000.

Gabrovšek, F., and W. Dreybrodt, A model of the early evolution of karst aquifers in limestone in the dimensions of length and depth, *J. Hydrol.*, *240*, 206–224, 2001.

Groves, C. G., and A. D. Howard, Minimum hydrochemical conditions allowing limestone cave development, *Water Resour. Res.*, *30*(3), 607–615, 1994a.

Groves, C. G., and A. D. Howard, Early development of karst systems, 1, Preferential flow path enlargement under laminar flow, *Water Resour. Res.*, *30*(10), 2837–2846, 1994b.

Horlacher, H.-B., and H.-J. Lüdecke, *Strömungsberechnung für Rohrsysteme*, Expert Verlag, Ehningen b. Böblingen, Germany, 1992.

Howard, A. D., and C. G. Groves, Early development of karst systems, 2, Turbulent flow, *Water Resour. Res.*, *31*(1), 19–26, 1995.

Hückinghaus, D., Simulation der Aquifergenese und des Wärmetransports in Karstsystemen, Ph.D. thesis, Fac. of Geosci., Univ. of Tübingen, Tübingen, Germany, 1998.

Jeannin, P.-Y., and J.-C. Maréchal, Lois de pertes de charge dans les conduits karstiques: Base théorique et observations, *Bull. Hydrogéol.*, *14*, 149–176, 1995.

Kaufmann, G., and J. Braun, Karst aquifer evolution in fractured rocks, *Water Resour. Res.*, *35*(11), 3023–3238, 1999.

Kaufmann, G., and J. Braun, Karst aquifer evolution in fractured, porous rocks, *Water Resour. Res.*, *36*(6), 1381–1391, 2000.

Kaye, C. A., The effect of solvent motion on limestone solution, *J. Geol.*, *65*, 35–46, 1957.

Kiraly, L., Régularisation de l'Areuse (Jura Suisse) simulée par modèle mathématique, in *Hydrogeology of karstic terraines*, edited by A. Burger and L. Dubertret, pp. 94–99, Heise, Hannover, Germany, 1984.

Lauritzen, S.-E., N. Odling, and J. Pedersen, Modelling the evolution of channel networks in carbonate rocks, in *Rock Characterization: ISRM Symposium, Eurock '92*, pp. 57–62, Br. Geotech. Soc., London, 1992.

Liedl, R., and M. Sauter, Modelling of aquifer genesis and heat transport in karst systems, *Bull. Hydrogéol.*, *16*, 185–200, 1998.

MacQuarrie, K. T. B., and E. A. Sudicky, On the incorporation of drains into three-dimensional variably saturated groundwater flow models, *Water Resour. Res.*, *32*(2), 477–482, 1996.

McDonald, M. G., and A. W. Harbaugh, A modular three-dimensional finite-difference ground-water flow model, *U.S. Geol. Surv. Techniques Water Resour. Invest., Bk. 6*, chap. A1, 1988.

Motyka, I., and Z. Wilk, Hydraulic structure of karst fissured Triassic rocks in the vicinity of Olkusz (Poland), *Kras Speleol.*, *145*, 11–24, 1984.

Palmer, A. N., Geomorphic interpretation of karst features, in *Groundwater as a Geomorphic Agent*, edited by R. G. LaFleur, pp. 173–209, Allen and Unwin, Concord Mass., 1984.

Palmer, A. N., Solutional enlargement of openings in the vicinity of hydraulic structures in karst regions, paper presented at 2nd Conference on Environmental Problems in Karst Terranes, Assoc. Groundwater Sci. and Eng., Dublin, Ohio, 1988.

Palmer, A. N., Origin and morphology of limestone caves, *Geol. Soc. Am. Bull.*, *103*, 1–21, 1991.

Palmer, A. N., Digital modeling of individual solution conduits, in *Speleogenesis—Evolution of Karst Aquifers*, edited by A. B. Klimchouk et al., pp. 194–200, Natl. Speleol. Soc., Huntsville, Ala., 2000.

Plummer, L. N., and T. M. L. Wigley, The dissolution of calcite in CO_2-saturated solutions at 25°C and 1 atm total pressure, *Geochim. Cosmochim. Acta*, *40*, 191–202, 1976.

Plummer, L. N., T. M. L. Wigley, and D. L. Parkhurst, The kinetics of calcite dissolution in CO_2-water systems at 5°C to 60°C and 0.0 to 1.0 atm CO_2, *Am. J. Sci.*, *278*, 179–216, 1978.

Press, W. H., B. P. Flannery, S. A. Teukolsky, and W. T. Vetterling, *Numerical Recipes in FORTRAN*, 963 pp., Cambridge Univ. Press, New York, 1992.

Sauter, M., Assessment of hydraulic conductivity in a karst aquifer at local and at regional scale, paper presented at 3rd Conference on Hydrogeology, Ecology, Monitoring and Management of Ground Water in Karst Terranes, U.S. Environ. Prot. Agency, Nashville, Tenn., 1991.

Sauter, M., Quantification and forecasting of regional groundwater flow and transport in a karst aquifer (Gallusquelle, Malm, SW Germany), *Tübinger Geowiss. Arb. C13*, 150 pp., Univ. of Tübingen, Tübingen, Germany, 1992.

Sauter, M., and R. Liedl, Modeling karst aquifer genesis using a coupled continuum-pipe flow model, in *Speleogenesis—Evolution of Karst Aquifers*, edited by A. B. Klimchouk et al., pp. 212–219, Natl. Speleol. Soc., Huntsville, Ala., 2000.

Siemers, J., and W. Dreybrodt, Early development of karst aquifers on percolation networks of fractures in limestone, *Water Resour. Res.*, *34*(3), 409–419, 1998.

Streeter, V. L., and E. B. Wylie, *Fluid Mechanics*, 564 pp., McGraw-Hill, New York, 1983.

Teutsch, G., Grundwassermodelle im Karst: Praktische Ansätze am Beispiel zweier Einzugsgebiete im Tiefen und Seichten Malmkarst der Schwäbischen Alb, 205 pp., Ph.D. thesis, Univ. of Tübingen, Tübingen, Germany, 1988.

Teutsch, G., Groundwater models in karstified terraines—Two practical examples from the Swabian Alb, S. Germany, paper presented at 4th Conference on Solving Groundwater Problems with Models, Int. Ground Water Model. Cent., Indianapolis, 1989.

Teutsch, G., and M. Sauter, Distributed parameter modelling approaches in karst-hydrological investigations, *Bull. Hydrogéol.*, *16*, 99–109, 1998.

Weyl, P. K., The solution kinetics of calcite, *J. Geol.*, *66*, 163–176, 1958.

White, W. B., Role of solutions kinetics in the development of karst aquifers, *Mem. Int. Assoc. Hydrogeol.*, *12*, 503–517, 1977.

White, W. B., Dissolution of limestone from field observations, in *Speleogenesis—Evolution of Karst Aquifers*, edited by A. B. Klimchouk et al., pp. 149–155, Natl. Speleol. Soc., Huntsville, Ala., 2000.

Yilin, C., W. Hongtao, and X. Xinhui, Dual-media flow models of karst areas and their application in north China, paper prestented at Karst Hydrogeology and Karst Environment Protection: 21st Congress of the International Association of Hydrogeologists, Int. Assoc. of Hydrogeol., Guilin, China, 1988.

Yusun, C., and B. Ji, The media and movement of karst water, paper prestented at Karst Hydrogeology and Karst Environment Protection: 21st Congress of the International Association of Hydrogeologists, Int. Assoc. of Hydrogeol., Guilin, China, 1988.

T. Clemens, D. Hückinghaus, R. Liedl, and G. Teutsch, Applied Geology, University of Tübingen, 72074 Tübingen, Germany. (rudolf.liedl@uni-tuebingen.de)

M. Sauter, Geoscience Centre, University of Göttingen, 37077 Göttingen, Germany.